













Article

Temporal Changes in the Infrared Spectra of Magellanic Carbon Stars

G. C. Sloan^{1,2,*}, K. E. Kraemer³, B. Aringer⁴, J. Cami^{5,6}, K. Eriksson⁷, S. Höfner⁷, E. Lagadec⁸, M. Matsuura⁹, I. McDonald¹⁰, E. Montiel¹¹, R. Sahai¹² and A. A. Zijlstra¹⁰

- ¹ Space Telescope Science Institute, 3700 San Martin Drive, Baltimore, MD 21218, USA
² Department of Physics and Astronomy, University of North Carolina, Chapel Hill, NC 27599-3255, USA
³ Institute for Scientific Research, Boston College, 140 Commonwealth Avenue, Chestnut Hill, MA 02467, USA
⁴ Department of Astrophysics, University of Vienna, Türkenschanzstraße 17, 1180 Wien, Austria
⁵ Department of Physics and Astronomy, The University of Western Ontario, London, ON N6A 3K7, Canada
⁶ Institute for Earth and Space Exploration, The University of Western Ontario, London, ON N6A 3K7, Canada
⁷ Theoretical Astrophysics, Department of Physics and Astronomy, Uppsala University, Box 516, 751 20 Uppsala, Sweden
⁸ Observatoire de la Côte d’Azur, CNRS, Laboratoire Lagrange, Université Côte d’Azur, Bd de l’Observatoire, CS 34229, 06304 Nice Cedex 4, France
⁹ Cardiff Hub for Astrophysical Research and Technology (CHART), School of Physics and Astronomy, Cardiff University, The Parade, Cardiff CF24 3AA, UK
¹⁰ Jodrell Bank Centre for Astrophysics, The University of Manchester, Manchester, M13 9PL, UK
¹¹ SOFIA-USRA, NASA Ames Research Center, MS 232-12, Moffett Field, CA 94035, USA
¹² Jet Propulsion Laboratory, MS 183-900, California Institute of Technology, Pasadena, CA 91109, USA
* Correspondence: gcsloan@stsci.edu

Abstract: The Medium-Resolution Spectrometer on the Mid-Infrared Instrument on the JWST obtained spectra of three carbon stars in the Large Magellanic Cloud. Two of the spectra differ significantly from spectra obtained ~16–19 years earlier with the Infrared Spectrograph on the Spitzer Space Telescope. The one semi-regular variable among the three has changed little. The long-period Mira variable in the sample shows changes consistent with its pulsation cycle. The short-period Mira shows dramatic changes in the strength of its molecular absorption bands, with some bands growing weaker and some stronger. Whether these variations result from its pulsation cycle or its evolution is not clear.

Keywords: stars: carbon; stars: AGB and post-AGB; circumstellar matter; dust



Citation: Sloan, G.C.; Kraemer, K.E.; Aringer, B.; Cami, J.; Eriksson, K.; Höfner, S.; Lagadec, E.; Matsuura, M.; McDonald, I.; Montiel, E.; Sahai, R.; Zijlstra, A.A. Temporal Changes in the Infrared Spectra of Magellanic Carbon Stars. *Galaxies* **2024**, *12*, 61. <https://doi.org/10.3390/galaxies12050061>

Academic Editor: Margo Aller

Received: 12 September 2024

Revised: 27 September 2024

Accepted: 1 October 2024

Published: 9 October 2024



Copyright: © 2024 by the authors. Licensee MDPI, Basel, Switzerland. This article is an open access article distributed under the terms and conditions of the Creative Commons Attribution (CC BY) license (<https://creativecommons.org/licenses/by/4.0/>).

1. Introduction

Carbon stars form when intermediate-mass stars on the asymptotic giant branch (AGB) dredge up enough freshly fused carbon from their interiors to push the C/O ratio in their envelopes past unity [1,2]. They dominate the dust production in the metal-poor Magellanic Clouds [3–5], likely making them an important contributor to dust in young galaxies at high redshifts. To understand how these stars produce dust, it is necessary to understand the chemistry and physics of the carbon-bearing molecules in their envelopes and how those molecules condense into carbon-rich dust.

The Spitzer Space Telescope obtained infrared spectra of 144 carbon stars in the Large Magellanic Cloud (LMC; see [6] and references therein). The majority of those spectra were observed with the low-resolution modules on the Infrared Spectrograph (IRS) [7] on the Spitzer Space Telescope [8], which covered the 5–14 μm region for the fainter targets observed, and extended to ~37 μm for the brighter targets. The spectral resolving power ($\lambda/\Delta\lambda$) varied between 64 and 128, depending on wavelength, which was sufficient for studying solid-state emission features from dust grains and the strength and general profile of molecular absorption bands.

The Medium-Resolution Spectrograph (MRS) [9] on the Mid-Infrared Instrument (MIRI) [10] aboard the James Webb Telescope [11] provides a spectral resolving power between 2000 and 3000 and can resolve the line structure within the absorption bands. We obtained time on JWST to observe nine carbon stars in the Magellanic Clouds with the MRS (Program 3010). The primary objective was to measure the resolved line structure to disentangle which molecules are responsible for the absorption at different wavelengths and to model the temperature and density of the absorbing gas.

This paper concentrates on the three spectra obtained prior to the Torino XIV AGB Workshop in 2024 June. Ultimately, this project will investigate the rich molecular content in the spectral data, but this paper focuses on the first surprise, that two of the three spectra obtained so far have changed significantly since they were observed with the IRS.

2. The Sample

Figure 1 shows the full sample of nine carbon stars in our program and the three stars observed with the MRS between 2023 November and 2024 March. Table 1 provides some background information on the three stars observed early; they are the focus of this paper. The target 2MASS J05062960–6855348 will be referred to as “J050629” hereafter. The nine stars in the full sample were selected to sample two sequences revealed in infrared color-color space. Figure 1 clearly separates the semi-regular variables (SRVs), which tend to be blue in most infrared colors, from the redder Miras. The MRS sample includes three targets on the SRV sequence and six on the Mira sequence.

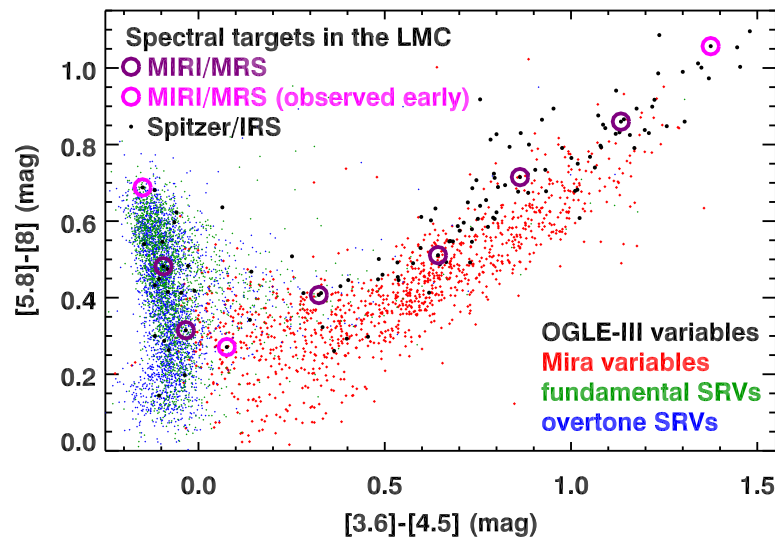


Figure 1. The sample of carbon stars observed with the MRS in the JWST program 3010 on an infrared color-color plot. The underlying photometry is from WISE and Spitzer, coded by variability classes from OGLE III. The three targets observed early (prior to 2024 June) are, from left to right, J050629, WBP 29, and MSX LMC 736.

Table 1. The first 3 carbon stars in the MRS sample.

Target	Period (Days)	[3.6]–[4.5] (mag)	[5.8]–[8] (mag)	IRS Epoch MJD ¹	MRS Epoch MJD ¹	Δt (yr) ²
J050629	154	−0.150	0.688	54,485	60,273	15.8
WBP 29	246	0.076	0.271	53,483	60,274	18.6
MSX LMC 736	690	1.375	1.057	54,611	60,385	15.8

¹ Modified Julian Date. ² Time between IRS and MRS observations.

All of the photometry in Figure 1 are from the Infrared Array Camera on Spitzer (IRAC) [12] and the Wide-field Infrared Survey Explorer (WISE) [13], supplemented with additional epochs obtained from the Near-Earth Object WISE Reactivated mission (NEOWISE-R) [14]. The IRAC data come from the SAGE survey of the LMC (Surveying

the Agents of a Galaxy’s Evolution) [15] and its follow-up to study variability in the core of the LMC (SAGE-Var) [16]. In Figure 1, the WISE data at 3.4 and 4.6 μm were shifted to the IRAC filters (3.6 and 4.5 μm) using the color-based corrections from [6]. The photometry for all available epochs are averaged after color correction.

The base sample in Figure 1 includes all SRVs and Mira variables identified in the LMC by the OGLE-III survey (Optical Gravitational Lensing Experiment) [17]. Figure 1 appeared in its original form for the SMC [18]. While the details differ in the two galaxies, most likely due to their different metallicities, both show the same striking dichotomy, with the SRVs and Miras clearly divided by [3.6]–[4.5] color. The pulsational properties of the stars are linked to the quantity and chemistry of the dust they produce [19]. The weakly pulsating SRVs produce small quantities of dust, much of it SiC, while the strong pulsations of the Miras result in higher dust-production rates dominated by amorphous carbon.

The full MRS sample follows the two sequences defined by the SRVs and Miras. While the SRVs tend to be blue in most infrared colors, the [5.8]–[8] color stands out as an exception. Because the stars are relatively dust-free, deep molecular bands can influence their color. The culprit is likely to be C_3 at $\sim 5 \mu\text{m}$ with a possible contribution from CO, which has a bandhead at 4.6 μm [18].

3. Spectra from the MRS on the JWST

Each MRS target was observed in all three grating settings to produce a continuous spectrum from 5 to 28 μm , although the quality of the data deteriorates past $\sim 20 \mu\text{m}$, due to dropping sensitivity and, for the bluer stars in the sample, decreasing signal from the target itself. The spectra in Figure 2 were produced by the default JWST pipeline [20], which does not include a correction for the residual fringing. The spectrophotometric calibration of the MRS agrees with the IRS on Spitzer to $\sim 2\%$ or better [21].

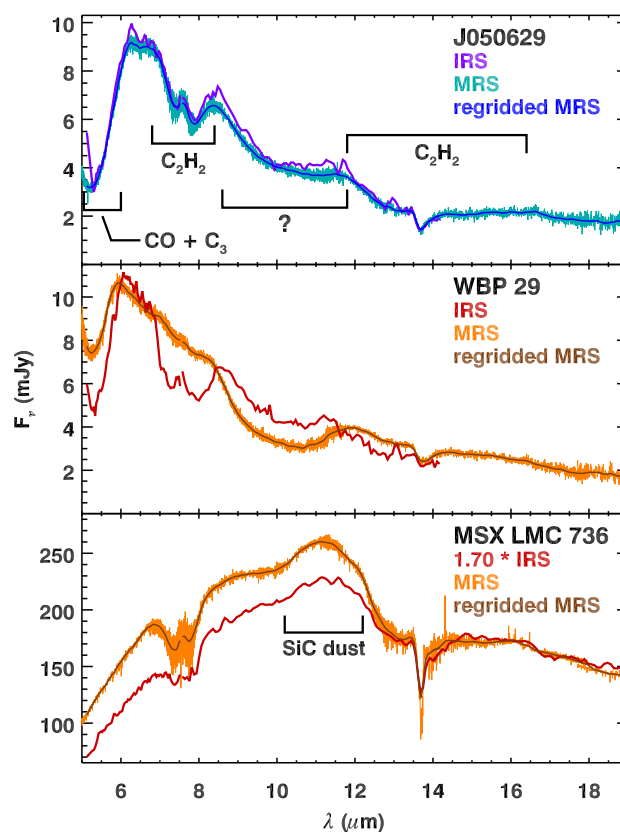


Figure 2. MRS spectra of the three targets observed prior to 2024 June compared to the spectra from the IRS. The spectra from the MRS are also plotted after downsampling them to the lower-resolution wavelength grid for the IRS. For MSX LMC 736, the IRS spectrum has been multiplied by 1.7 to align it to the MRS data at 17 μm for easier comparison.

For each source, Figure 2 shows a spectrum from the MRS at its full resolution, a spectrum of the same target obtained ~16–19 years earlier with the IRS on Spitzer (see [6] for details of the IRS observations), and the MRS data resampled to the IRS wavelength grid. While some residual fringes remain in the MRS data, nearly all of the detailed structure in the full-resolution spectrum is the actual line structure within the molecular bands. The apparent position of the “continuum” in the downsampled version of the MRS spectrum demonstrates the challenge of determining the actual continuum in these complex spectra.

4. Light Curves and Pulsation Periods

For each target, we used the multi-epoch photometry from the SAGE surveys at 3.6 and 4.5 μm and WISE at 3.4 and 4.6 μm to construct light curves. The IRAC data were shifted to the WISE filters using color corrections algebraically determined from those provided by [6].

Table 1 gives the pulsation periods for the three stars investigated here. For the two bluer sources, we used the periods provided by previous surveys. The period of 154 d for J050629 comes from OGLE III [17], but OGLE III also suggested a period of 741 d with a slightly higher amplitude. The MACHO survey (the survey for Massive Compact Halo Objects) [22] fitted two periods with similar amplitudes: 267 d and 238 d. None of these alternate periods fits the WISE and IRAC photometry for J050629 particularly well. For WBP 29, we took the average from the MACHO and OGLE-III surveys (246 and 247 d, respectively).

The light curves for J050629 and WBP 29 reveal a problem with our conversions of the IRAC photometry at 3.6 and 4.5 μm to the WISE filters centered at 3.4 and 4.6 μm . The supposedly corrected IRAC photometry is roughly 0.2 magnitudes brighter than the WISE photometry. A comparison of contemporaneous data at MJD \sim 55,400 shows the issue most clearly. The probable cause of the discrepancy is the molecular band absorption affecting wavelengths outside the region of overlap in the two filter sets. We did not use the IRAC photometry when fitting light curves for these two sources.

For both J050629 and WBP 29, the adopted period was fitted to the WISE data with a sine function to determine the zero-phase epoch and amplitude for the two filters. The zero-phase epoch was then averaged between the two filters to produce the light curves in Figure 3. As explained in the next section, the estimated phases for the MRS and IRS epochs are not reliable for J050629 and are uncertain for WBP 29.

The OGLE-III survey is biased against the carbon stars most deeply embedded within their own dust shells, because the dust extinction makes them too faint to be detected in the optical. The result can be seen in Figure 1, where the OGLE-based sample fades away at the reddest colors, even though plenty of targets were still observed by the IRS on Spitzer.

Our reddest target, MSX LMC 736, is not in the OGLE-III sample, so we determined a pulsation period of 690 d from the multi-epoch WISE and (filter-corrected) IRAC data using the minimization algorithm described by [6]. In brief, that algorithm iterates through periods, fits an amplitude and zero-phase epoch to the photometry at each period, and returns the period with the smallest root-mean-squared residuals. The result was consistent for both WISE filters and with and without the IRAC epochs (689.7 to 690.3 d). Previous efforts using similar data and methods produced periods of 686 d [6] and 683 d [23]. The differences likely arise from fewer epochs available previously. Using completely independent data from the VISTA Magellanic Cloud survey, Ref. [24] found a period of 672 d. The differences between these reported periods give some idea of the overall uncertainties. Using a period of 690 d, a light curve was fitted to the available data as with the other two targets. For MSX LMC 736, the color-corrected IRAC data were also used.

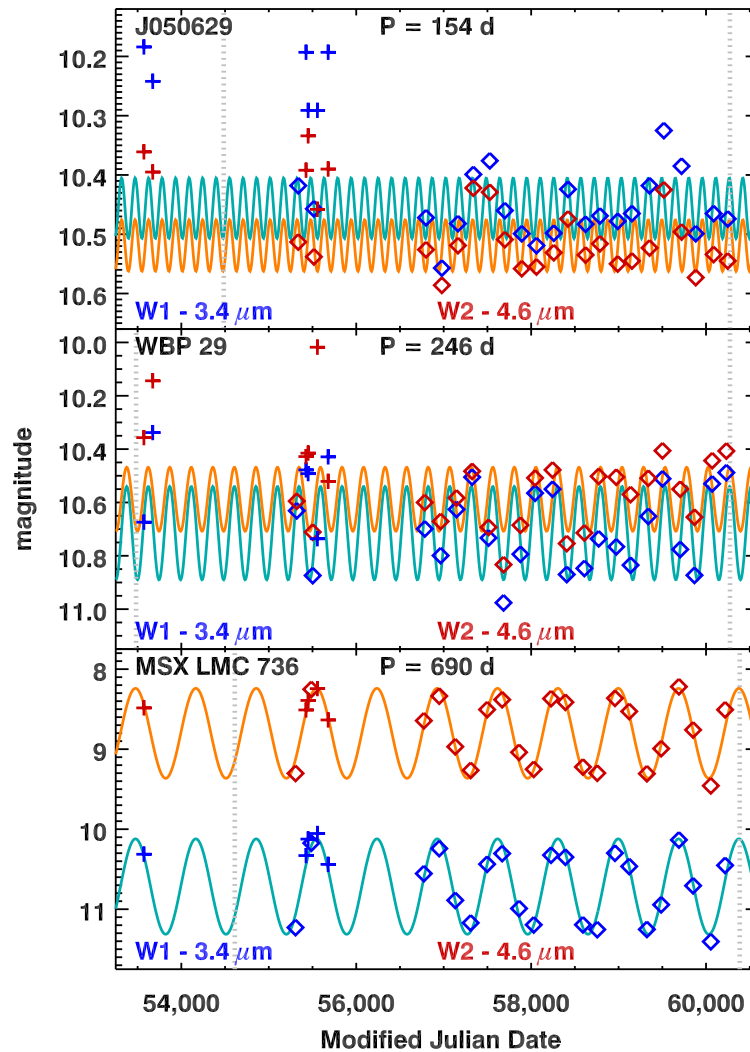


Figure 3. Light curves for the three targets in the current sample. The vertical dashed lines for each target mark the times they were observed by the IRS on Spitzer (left) and the MRS on the JWST (right). WISE data are plotted as diamonds, and IRAC data (after conversion to the WISE filters) are plotted as plus signs. The orange and light blue curves are fitted to the red and blue data, respectively, as explained in the text. Section 5 discusses the reliability of the estimated phases for the MRS and IRS observing epochs for the three targets.

5. Discussion

5.1. J050629

J050629 is the bluest target in [3.6]–[4.5] of the nine in the full MRS sample. Of the three SRVs, it is the reddest in the [5.8]–[8] color, and Figure 2 shows why. It has strong C_3 and CO absorption at $5 \mu\text{m}$, and that is affecting the measured [5.8]–[8].

The spectrum of J050629 has changed little between the IRS and MRS epochs. Both epochs show an absorption band at $5 \mu\text{m}$. Both spectra also show an acetylene (C_2H_2) band at $7.5 \mu\text{m}$ with its characteristic “W” shape. A second acetylene band appears at $13.7 \mu\text{m}$, or more properly, the Q branch of a wider band that stretches from ~ 12.5 to $16 \mu\text{m}$. A broad, smooth absorption band from an unknown carrier is also present, centered at $\sim 10 \mu\text{m}$. A dust emission feature from SiC could be present at $\sim 11.5 \mu\text{m}$, but this apparent emission feature could just be the continuum between the two broad absorption bands to either side. The most notable differences between the two spectra can be attributed to noise in the IRS data.

While the light curve for J050629 suggests that the IRS observed it at minimum and the MRS observed it 15.8 years later at maximum, the short pulsation period should limit

confidence in that conclusion. The pulsation period is only 154 d, implying 37.4 pulsation cycles between the spectral epochs. Just a two-day shift in pulsation period would be sufficient to add half a pulsation cycle in 15.8 years, which would place both spectral observations at the same pulsation phase. Given that the star is a semi-regular variable, such a small shift seems entirely possible.

5.2. MSX LMC 736

MSX LMC 736 is the reddest target in [3.6]–[4.5] in the full MRS sample due to the large quantity of amorphous carbon dust in its circumstellar shell. Its light curve shows strong pulsations, with peak-to-peak amplitudes > 1.0 magnitude in both filters. Its spectrum shows both acetylene bands, centered at 7.5 and 13.7 μm , as well as an unambiguous SiC dust emission feature at $\sim 11.5 \mu\text{m}$.

The MRS spectrum is 70% brighter than the IRS spectrum, if one compares the two at 17 μm , but the MRS spectrum is even brighter in the 5–12 μm range, suggesting a higher fraction of warm dust. The long and steady pulsation period of MSX LMC 736 (Figure 3) results in a well-fitted light curve that shows clearly that the IRS data were obtained close to minimum and the MRS data close to maximum. The long pulsation period and the excellent agreement between the photometry and a sinusoidal model give us confidence in this conclusion. The changes in the spectrum are consistent with the star's pulsation cycle, with the MRS data obtained during a phase of higher luminosity of the central star, leading to higher atmospheric temperatures and warmer dust.

5.3. WBP 29

Of the three stars in the sample observed before the Torino XIV AGB meeting, WBP 29 is the enigma. While the spectra from the IRS and MRS have roughly the same brightness outside of the deeper molecular bands, the bands have changed dramatically between the two epochs. In the MRS spectrum, the C_3 and CO absorption at 5 μm have been cut in half, while the 7.5 μm acetylene band has nearly vanished. In its place is a much stronger absorption band from an unknown carrier centered at 10 μm (like the band in J050629, but stronger). The low S/N at 14 μm in the IRS data limits comparisons of the 13.7 μm acetylene band. The MRS data show a hint of what could be SiC dust emission at 11.5 μm , but in all likelihood, that is just continuum.

WBP 29 is the bluest of the six Miras and closest to the boundary with the SRVs. Its relatively blue color for a Mira indicates that it has not yet produced a lot of dust, and that suggests that it may be in the process of shifting from an SRV, as the amplitude of the fundamental pulsation mode grows and begins to dominate the overtone modes. As the authors of [19] have shown, this shift is associated with an increase in the dust-production rate for amorphous carbon. In this context, the changes in the molecular chemistry could provide clues about how the circumstellar envelope is changing as the star passes through this transition to Mira. This possibility was raised at the Torino XIV AGB meeting.

If the phase information in the fitted light curve is reliable, then the IRS spectrum was obtained at minimum and the MRS spectrum at maximum. That would mean that the spectral variations seen could be due primarily to the pulsation cycle. However, the light curve fitted to the data for WBP 29 in Figure 3 is not conclusive, and further analysis is needed for any certainty in the phases of the IRS and MRS observations. Whatever the cause of the differences in the spectra, the molecular chemistry has clearly changed.

6. Conclusions

This short contribution describes the first three spectra obtained out of nine in the total sample. The analysis here focuses on the overall shape of the molecular bands and dust features. These new data demonstrate that temporal information is an important part of any study of carbon stars, due to their pulsations and dynamic behavior. The molecular component in the new MRS data was the original objective of this project, and the data

promise to reveal a great deal more about carbon stars as they evolve and ultimately eject their envelopes.

Author Contributions: G.C.S. led the writing of the JWST observing proposal, the reduction and analysis of the data, and the preparation of this manuscript. K.E.K. assisted with the preparation of the first draft. All of the coauthors reviewed and edited the original observing proposal and reviewed and edited this manuscript. All authors have read and agreed to the published version of the manuscript.

Funding: K.K., E.M., R.S., and G.S. are supported by subawards from the Guest-Observer award JWST-GO-03010 provided by the Space Telescope Science Institute. R.S.'s contribution was carried out at the Jet Propulsion Laboratory, California Institute of Technology, under a contract with NASA. These results are based on observations with the NASA/ESA/CSA James Webb Space Telescope, which is operated at the Space Telescope Science Institute by the Association of Universities for Research in Astronomy, Incorporated, under NASA contract NAS5-03127. Support for Program number (STScI Program Number) was provided through a grant from the STScI under NASA contract NAS5-03127. J.C. acknowledges the support of the Natural Sciences and Engineering Research Council (NSERC) of Canada. S.H. acknowledges funding from the European Research Council (ERC) under the European Union's Horizon 2020 research and innovation program (grant agreement No. 883867, project EXWINGS) and the Swedish Research Council (Vetenskapsrådet, grant number 2019-04059). M.M. acknowledges support from the STFC Consolidated grant (ST/W000830/1). This publication is based on work from COST Action CA21126—Carbon molecular nanostructures in space (NanoSpace), supported by COST (European Cooperation in Science and Technology).

Data Availability Statement: The spectroscopic data from MIRI will be available from mast.stsci.edu at the end of their one-year proprietary period. The spectroscopic data from Spitzer and the photometric data used in this work are on publicly available archives.

Acknowledgments: The authors thank the anonymous reviewers for helpful guidance on improving this paper.

Conflicts of Interest: The authors declare that they have no conflicts of interest.

References

1. Habing, H.J. Circumstellar envelopes and Asymptotic Giant Branch stars. *Astron. Astrophys. Rev.* **1996**, *7*, 97–207. [[CrossRef](#)]
2. Höfner, S.; Olofsson, H. Mass loss of stars on the asymptotic giant branch. Mechanisms, models and measurements. *Astron. Astrophys. Rev.* **2018**, *26*, 1. [[CrossRef](#)]
3. Boyer, M.L.; Srinivasan, S.; Riebel, D.; McDonald, I.; Van Loon, J.T.; Clayton, G.C.; Gordon, K.D.; Meixner, M.; Sargent, B.A.; Sloan, G.C. The dust budget of the Small Magellanic Cloud: Are asymptotic giant branch stars the primary dust source at low metallicity? *Astrophys. J.* **2012**, *748*, 40. [[CrossRef](#)]
4. Matsuura, M.; Barlow, M.J.; Zijlstra, A.A.; Whitelock, P.A.; Cioni, M.R.; Groenewegen, M.A.T.; Volk, K.; Kemper, F.; Kodama, T.; Lagadec, E.; et al. The global gas and dust budget of the Large Magellanic Cloud: AGB stars and supernovae, and the impact on the ISM evolution. *Mon. Not. R. Astron. Soc.* **2009**, *396*, 918–934. [[CrossRef](#)]
5. Matsuura, M.; Woods, P.M.; Owen, P.J. The global gas and dust budget of the Small Magellanic Cloud. *Mon. Not. R. Astron. Soc.* **2013**, *429*, 2527–2536. [[CrossRef](#)]
6. Sloan, G.C.; Kraemer, K.E.; McDonald, I.; Groenewegen, M.A.T.; Wood, P.R.; Zijlstra, A.A.; Lagadec, E.; Boyer, M.L.; Kemper, F.; Matsuura, M.; et al. The infrared spectral properties of Magellanic carbon stars. *Astrophys. J.* **2016**, *826*, A44. [[CrossRef](#)]
7. Houck, J.R.; Roellig, T.L.; van Cleve, J.; Forrest, W.J.; Herter, T.; Lawrence, C.R.; Matthews, K.; Reitsema, H.J.; Soifer, B.T.; Watson, D.M.; et al. The Infrared Spectrograph (IRS) on the Spitzer Space Telescope. *Astrophys. J. Suppl. Ser.* **2004**, *158*, 18–24. [[CrossRef](#)]
8. Werner, M.W.; Roellig, T.L.; Low, F.J.; Rieke, G.H.; Rieke, M.; Hoffmann, W.F.; Cruikshank, D.P. The Spitzer Space Telescope mission. *Astrophys. J. Suppl. Ser.* **2004**, *154*, 1–9. [[CrossRef](#)]
9. Wells, M.; Pels, J.-W.; Glasse, A.; Wright, G.S.; Aitink-Kroes, G.; Azzollini, R.; Beard, S.; Brandl, B.R.; Gallie, A.; Geers, V.C.; et al. The mid-infrared instrument for the James Webb Space Telescope, VI: The medium resolution spectrometer. *Publ. Astron. Soc. Pac.* **2015**, *127*, 646–664. [[CrossRef](#)]
10. Wright, G.S.; Rieke, G.H.; Glasse, A.; Ressler, M.; Marín, M.G.; Aguilar, J.; Alberts, S.; Álvarez-Márquez, J.; Argyriou, I.; Banks, K.; et al. The Mid-infrared Instrument for JWST and its in-flight performance. *Publ. Astron. Soc. Pac.* **2024**, *135*, A48003.
11. Gardner, J.P.; Mather, J.C.; Abbott, R.; Abell, J.S.; Abernathy, M.; Abney, F.E.; Abraham, J.G.; Abraham, R.; Abul-Huda, Y.M.; Acton, S.; et al. The James Webb Space Telescope mission. *Publ. Astron. Soc. Pac.* **2023**, *135*, A68001. [[CrossRef](#)]
12. Fazio, G.G.; Hora, J.L.; Allen, L.E.; Ashby, M.L.N.; Barmby, P.; Deutsch, L.K.; Huang, J.S.; Kleiner, S.; Marengo, M.; Megeath, S.T.; et al. The Infrared Array Camera (IRAC) for the Spitzer Space Telescope. *Astrophys. J. Suppl. Ser.* **2004**, *154*, 10–17. [[CrossRef](#)]

13. Wright, E.L.; Eisenhardt, P.R.M.; Mainzer, A.K.; Ressler, M.E.; Cutri, R.M.; Jarrett, T.; Kirkpatrick, J.D.; Padgett, D.; McMillan, R.S.; Skrutskie, M.; et al. The Wide-field Infrared Survey Explorer (WISE): Mission description and initial on-orbit performance. *Astron. J.* **2010**, *140*, 1868–1881. [[CrossRef](#)]
14. Mainzer, A.; Bauer, J.; Cutri, R.M.; Grav, T.; Masiero, J.; Beck, R.; Clarkson, P.; Conrow, T.; Dailey, J.; Eisenhardt, P.; et al. Initial performance of the NEOWISE Reactivation mission. *Astrophys. J.* **2014**, *792*, 30. [[CrossRef](#)]
15. Meixner, M.; Gordon, K.D.; Indebetouw, R.; Hora, J.L.; Whitney, B.; Blum, R.; Reach, W.; Bernard, J.P.; Meade, M.; Babler, B.; et al. Spitzer Survey of the Large Magellanic Clouds: Surveying the Agents of a Galaxy’s Evolution (SAGE). I. Overview and initial results. *Astron. J.* **2006**, *132*, 2268–2288. [[CrossRef](#)]
16. Riebel, D.; Boyer, M.L.; Srinivasan, S.; Whitelock, P.; Meixner, M.; Babler, B.; Feast, M.; Groenewegen, M.A.T.; Ita, Y.; Meade, M.; et al. SAGE-Var: An infrared survey of variability in the Magellanic Clouds. *Astrophys. J.* **2015**, *807*, 1. [[CrossRef](#)]
17. Soszyński, I.; Udalski, A.; Szymański, M.K.; Kubiak, M.; Pietrzyński, G.; Wyrzykowski, L.; Szewczyk, O.; Ulaczyk, K.; Poleski, R. The Optical Gravitational Lensing Experiment. The OGLE-III Catalog of Variable Stars. IV. Long-period variables in the Large Magellanic Cloud. *Acta Astron.* **2009**, *59*, 239–253.
18. Sloan, G.C.; Lagadec, E.; Kraemer, K.E.; Boyer, M.L.; Srinivasan, S.; McDonald, I.; Zijlstra, A.A. The properties of carbon stars in the Small Magellanic Cloud. In *Why Galaxies Care about AGB Stars*, 3rd ed.; Kerschbaum, F., Hron, J., Wing, R., Eds.; Springer: Berlin/Heidelberg, Germany, 2014; Volume 497; p. 429.
19. Kraemer, K.E.; Sloan, G.C.; Keller, L.D.; Forrest, W.J.; Herter, T.; Lawrence, C.R.; Matthews, K.; Reitsema, H.J.; Soifer, B.T.; Watson, D.M.; et al. Stellar pulsation and the production of dust and molecules in Galactic carbon stars. *Astrophys. J.* **2019**, *887*, 82. [[CrossRef](#)]
20. Bushouse, H.; Eisenhamer, J.; Dencheva, N.; Davies, J.; Greenfield, P.; Morrison, J.; Hodge, P.; Simon, B.; Grumm, D.; Droettboom, M.; et al. JWST Calibration Pipeline, Version 1.14.0, Computer Software. *Zenodo*, 25 March 2024. [[CrossRef](#)]
21. Law, D.R.; Argyriou, I.; Gordon, K.D.; Sloan, G.C.; Gasman, D.; Glasse, A.; Larson, K.; Fletcher, L.N.; Labiano, A.; Noriega-Crespo, A.; et al. The James Webb Space Telescope absolute flux calibration. III. Mid-Infrared Instrument Medium Resolution IFU Spectrometer. *arXiv* **2024**, arXiv:2409.15435.
22. Fraser, O.J.; Hawley, S.L.; Cook, K.H.; Keller, S.C. Long-period variables in the Large Magellanic Cloud: Results from MACHO and 2MASS. *Astron. J.* **2005**, *129*, 768–775. [[CrossRef](#)]
23. Groenewegen, M.A.T.; Sloan, G.C. Luminosities and mass-loss rates of Local Group AGB stars and red supergiants. *Astron. Astrophys.* **2018**, *609*, A114. [[CrossRef](#)]
24. Groenewegen, M.A.T.; Nanni, A.; Cioni, M.-R.L.; Girardi, L.; De Grijs, R.; Ivanov, V.D.; Marconi, M.; Moretti, M.I.; Oliveira, J.M.; Petr-Gotzens, M.G.; et al. The VMC Survey. XXXVII. Pulsation periods of dust-enshrouded AGB stars in the Magellanic Clouds. *Astron. Astrophys.* **2020**, *636*, A48. [[CrossRef](#)]

Disclaimer/Publisher’s Note: The statements, opinions and data contained in all publications are solely those of the individual author(s) and contributor(s) and not of MDPI and/or the editor(s). MDPI and/or the editor(s) disclaim responsibility for any injury to people or property resulting from any ideas, methods, instructions or products referred to in the content.